JOURNAL OF BACTERIOLOGY, May 2005, p. 3496–3501 Vol. 187, No. 10
0021-9193/05/$08.00+0 doi:10.1128/JB.187.10.3496–3501.2005

Solution Structure of the Carbon Storage Regulator Protein CsrA from *Escherichia coli*

Pablo Gutiérrez, Yan Li, Michael J. Osborne, Ekaterina Pomerantseva, Qian Liu, and Kalle Gehring*

Department of Biochemistry, McGill University, 3655 Promenade Sir William Osler, Montreal, Quebec, Canada H3G 1Y6

Received 14 November 2004/Accepted 11 February 2005

The carbon storage regulator A (CsrA) is a protein responsible for the repression of a variety of stationary-phase genes in bacteria. In this work, we describe the nuclear magnetic resonance (NMR)-based structure of the CsrA dimer and its RNA-binding properties. CsrA is a dimer of two identical subunits, each composed of five strands, a small α-helix and a flexible C terminus. NMR titration experiments suggest that the β1-β2 and β3-β4 loops and the C-terminal helix are important elements in RNA binding. Even though the β3-β4 loop contains a highly conserved RNA-binding motif, GxxG, typical of KH domains, our structure excludes CsrA from being a member of this protein family, as previously suggested. A mechanism for the recognition of mRNAs downregulated by CsrA is proposed.

Carbon storage regulator A (CsrA) is a central component of the global regulatory system Csr, which is responsible for the repression of a variety of stationary-phase genes (22). CsrA negatively regulates gluconeogenesis, glycogen biosynthesis and catabolism, and biofilm formation (14, 23, 25). Additionally, CsrA can activate glycolysis, acetate metabolism, and flagellum biosynthesis (25–27). CsrA acts posttranscriptionally by repressing gene expression of essential enzymes in carbohydrate metabolism, like ADP-glucose pyrophosphorylase (*glgC*), glycogen synthase (*glgA*), glycogen branching enzyme (*glgB*), and glycogen phosphorylase (*glgP*). CsrA destabilizes target mRNAs by binding in a region within the −18 and +31 nucleotides of the coding region, which includes the ribosome-binding site (18). This prevents translation of the corresponding mRNA and promotes its degradation by endogenous RNases. As a result, a decrease in the intracellular levels of the glycogen biosynthetic enzymes and decreased synthesis of intracellular glycogen are observed.

Intracellular levels of CsrA are regulated by two untranslated RNA molecules, CsrB and CsrC, that act as antagonists by sequestering CsrA and preventing its binding to target mRNAs (13, 17, 28). CsrA binding to both CsrB and CsrC seems to be mediated by a highly repetitive sequence element, 5′-CAGGA(U,C,A)G-3′, located in the loops of predicted CsrB/C hairpins (17, 28). It has been proposed that CsrA exists in equilibrium between CsrB/C and CsrA-regulated mRNAs, implying that CsrB/C levels are a key determinant of CsrA activity in the cell.

CsrA homologs have been recognized for important roles in the regulation of stationary-phase gene expression in other bacterial species. The CsrA homolog (RsmA) of *Erwinia* species regulates a variety of genes involved in soft-rot disease of higher plants (8, 9). *csrA* and *csrB* in *Salmonella enterica* serovar Typhimurium regulate genes involved in epithelial cell invasion by this species (2). In *Pseudomonas aeruginosa*, the Csr (Rms) system controls the quorum-sensing systems Las and Rhl, which regulate several of its virulence factors.

CsrA is a 61-amino-acid dimeric protein previously thought to be related to RNA-binding proteins containing the KH motif (18). In this work we describe a nuclear magnetic resonance (NMR)-based model of the CsrA dimer from *Escherichia coli* and some of its RNA-binding properties. Furthermore, a mechanism for the recognition of mRNAs down regulated by CsrA is discussed.

MATERIALS AND METHODS

Sample preparation. Gene *csrA* from *E. coli* K-12 was subcloned into pET15b (Novagen, Inc., Madison, WI) and expressed in *E. coli* BL21 as an oligo-histidine (His tag) fusion protein of 9 kDa. Cells were grown at 37°C to an optical density at 600 nm of 0.8 and induced with 1 mM isopropyl-β-D-thiogalactopyranoside. Afterwards, the temperature was reduced to 30°C and the cells were allowed to express the protein for 3 h before harvesting. The media used were either LB or M9 minimal medium containing [^{15}N]ammonium chloride and/or [^{13}C]glucose (Cambridge Isotopes Laboratory, Andover, MA). CsrA was purified by affinity chromatography on Ni^{2+}-loaded chelating Sepharose (Amersham Pharmacia Biotech, Piscataway, NJ). NMR samples were ~1 mM protein in 50 mM sodium acetate buffer, 300 mM NaCl at pH 4.5. For preparation of ^{13}C- and ^{15}N-labeled and unlabeled protein samples, equal amounts of purified ^{13}C- and ^{15}N-labeled and unlabeled proteins were mixed in the presence of 6 M urea overnight. Urea was removed by extensive dialysis against NMR buffer.

Gel filtration. The oligomeric state of CsrA was determined using gel filtration (Hiload 16/60 Superdex 75; Pharmacia Biotech). Regeneration-induced CNP homolog (RICH) (53.8 kDa), RICH in 1 mM dithiothreitol (26.9 kDa), and gamma-ear protein (13.8 kDa) were used as standards. Samples were run with a flow rate of 1 ml/min at room temperature in NMR buffer as described above. CsrA eluted from the column at a predicted molecular mass of ~18 kDa as expected for a dimer.

NMR spectroscopy. NMR experiments were recorded at 303 K on a Bruker Avance 600-MHz spectrometer. Backbone and side chain assignments of CsrA were determined in HNCACB, CBCA(CO)NH, edited [^{15}N/^{13}C]TOCSY-HMQC, [^{13}C]HCCH-TOCSY, and [^{13}C](h)CCH-TOCSY experiments. NOE data for the structure determination were obtained from homonuclear NOESY, ^{15}N-edited or ^{13}C-edited 3D NOESY experiments. Backbone assignments at pH 7.5 were determined using HNCA and CBCA(CO)NH experiments. The intermolecular NOEs were detected using a filter-edited 3D NOESY spectrum and a pair of identical ^{13}C-edited 3D NOESY with and without decoupling in the

* Corresponding author. Mailing address: Department of Biochemistry, McGill University, 3655 Promenade Sir William Osler, Montreal, Quebec, Canada H3G 1Y6. Phone: (514) 398-7287. Fax: (514) 398-7384. E-mail: kalle.gehring@mcgill.ca.

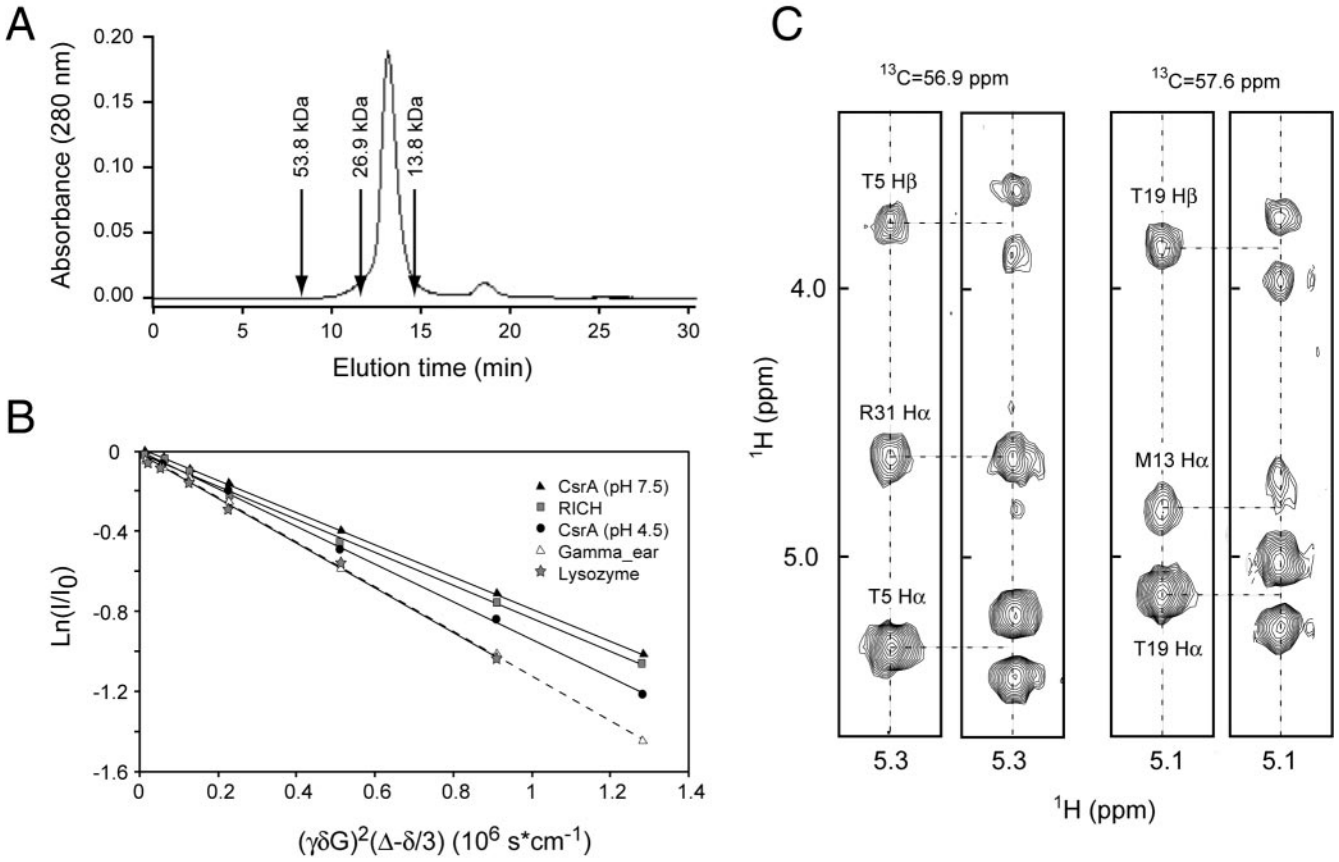

FIG. 1. Structure determination of the CsrA dimer. A. Gel filtration chromatogram of CsrA. Protein standards were RICH (53.8 kDa), RICH in 1 mM dithiothreitol (26.9 kDa), and gamma-adaptin ear protein (13.8 kDa) as indicated. CsrA eluted as an ~18-kDa protein, consistent with a dimeric form. B. Pulse-field gradient–self-diffusion experiments for CsrA. The slopes in the plot are proportional to the diffusion coefficient (D_s). C. Representative two-dimensional strips of ^{13}C edited NOESY experiments with and without carbon decoupling in a 1:1 sample of $^{13}C/^{15}N$-labeled/unlabeled protein. Peaks from the carbon-coupled experiment are shown to the left for both sets of strips. NOEs resulting from intermolecular interactions appear as singlets in both experiments, while intramolecular NOEs are doublets in the uncoupled experiment.

indirect ^1H dimension (100-ms mixing time). A $^{13}C/^{15}N$-labeled/nonlabeled protein sample (1:1) was used for these experiments. ^1H-^{15}N residual dipolar coupling constants were measured from comparison of IPAP-HSQC experiments recorded on CSRA with and without 2.5% C12E5–hexanol (24) For the measurement of dipolar couplings we used 50 mM sodium acetate buffer at pH 4.5 and 0.5 mM CSRA. All NMR spectra were processed using either XWINNMR version 2.5 or 3.1 (Bruker Biospin) or NMRPipe (10). Evaluation of spectra and manual assignments were completed with NMRView (15). Pulse-field gradient self-diffusion experiments were done according to the method reported by Ekiel et al. (12).

Structure calculations. CNS 1.1 software (4) was used to generate an initial fold of CsrA with a basic set of 122 NOEs manually assigned from NOESY spectra (104 intramolecular and sequential NOEs). Hydrogen bond constraints were introduced to secondary structure regions as determined by chemical shift analysis, characteristic NOE patterns, and analysis of amide exchange rates. Dihedral restraints (ϕ and ψ) were obtained using the TALOS program (7). These calculations generated a fold that was used as a model template for automated assignments by ARIA1.1 (21). The final structure of CsrA was calculated with a total set of 710 constraints collected from the experiments described earlier. Noncrystallographic symmetry restraints were used to keep both subunits in the dimer with the same conformation. In the final round of calculations, CNS 1.1 was extended to incorporate residual dipolar coupling (RDC) restraints for further refinement using the torsion angle space. The axial and rhombic components were defined from a histogram of measured RDCs (5) and optimized by a grid search method (6). Ten structures were selected based on the lowest overall energy and least violations to represent final structures. PROCHECK-NMR was used to generate Ramachandran plots to check the protein's stereochemical geometry (16). A summary of the structural statistics for CsrA is shown below in Table 1.

NMR titrations. RNA titrations were performed by recording a series of [^{15}N]HSQC spectra on uniformly ^{15}N-labeled CsrA (~0.7 mM CsrA) in the presence of different amounts of ligand concentrations in the 0 to 2.0 mM range. As high concentrations of imidazole improve the solubility of CsrA at physiological pH, the protein sample and RNA stock solutions were prepared in 500 mM deuterated imidazole, 300 mM NaCl at pH 7.5. The RNA sequences used were 5′-ACCUGCACACGGAUUGUGUGGUUC-3′ (glg25), 5′-CACACGGAUUGUGUG-3′ (glg15), and 5′-CAGGAUG-3′ (CsrB consensus sequence) and were synthesized in the Core DNA & Protein Services, University of Calgary.

Protein structure accession numbers. The coordinates of CsrA have been deposited in the RCSB under PDB code 1Y00, and the NMR assignments are under BMRB accession 11855.

RESULTS AND DISCUSSION

Structure determination of the CsrA dimer. Mass spectrometry of cross-linked CsrA demonstrated that CsrA exists in solution as a dimer of identical subunits (11). However, our preliminary work showed that CsrA aggregates at physiological pH at concentrations above 0.1 mM. At pH 7.5, size exclusion chromatography showed the presence of three peaks with apparent molecular masses of 18, 36, and 54 kDa compatible with

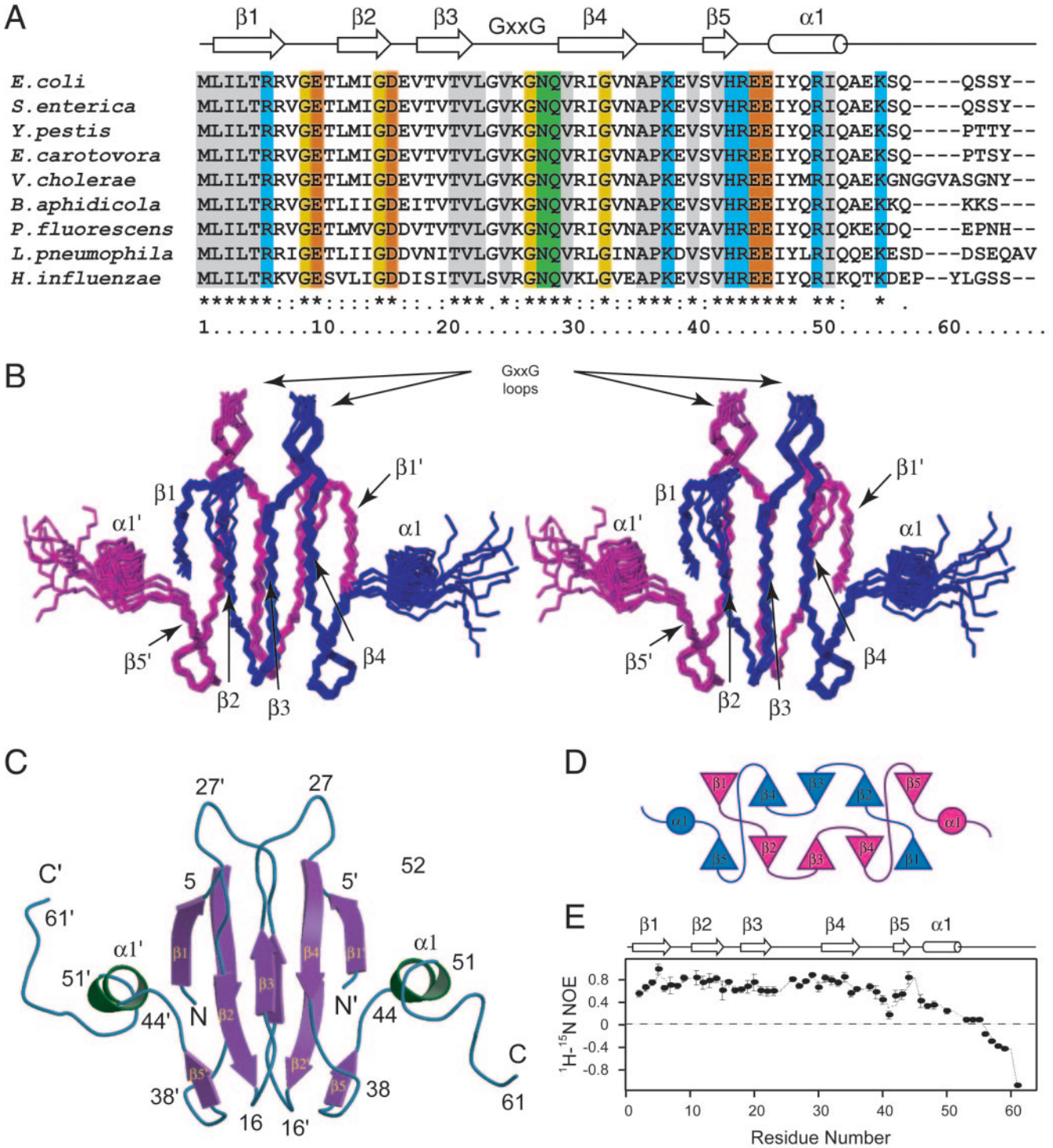

FIG. 2. Structure of CsrA. (A) The CsrA sequence from *E. coli* K-12 (gi:161306043) is aligned with homologous proteins from *S. enterica* (gi:16766132), *Yersinia pestis* (gi:16123457), *E. carotovora* (gi:50122288), *Vibrio cholerae* (gi:9654977), *Buchnera aphidicola* (gi:21672665), *Pseudomonas fluorescens* (gi:38489882), *Legionella pneumophila* (gi:54296805), and *Haemophilus influenzae* (gi:16272754). Completely conserved acidic, basic, polar, and hydrophobic residues are red, blue, green, and gray, respectively. The location of secondary structure elements is shown on top. (B) Stereo view of the backbone atoms for residues 1 to 55 of 10 selected conformers. The two subunits are magenta and blue. (C) Ribbon depiction of CsrA. (D) Topology diagram of the CsrA structure showing the connectivity between strands in the two β-sheets. (E) Values of the {^{1}H}-^{15}N heteronuclear NOE for backbone amides, showing the unstructured C terminus.

the formation of dimers, tetramers, and hexamers (data not shown). Size exclusion chromatography showed that at low pH (~4.5), CsrA does not aggregate into higher-order forms but remains as a dimer (Fig. 1A). Gel filtration data were also confirmed by NMR self-diffusion experiments (Fig. 1B) (12). At pH 4.5, CsrA had a diffusion coefficient of 0.93×10^6 cm^2/second, in agreement with the formation of a dimer at low pH (apparent molecular mass of 18.6 kDa). The apparent molecular mass for the aggregate at pH 7.5 was ~29.3 kDa. NMR experiments for determining the solution structure of CsrA were performed at pH 4.5.

CsrA was uniformly labeled with ^{15}N or doubly labeled with ^{15}N and ^{13}C for NMR analysis. Backbone resonance assignments were obtained with standard triple resonance NMR experiments. Chemical shift indices of Cα, Cβ, and Hα (29) and the analysis of sequential and short-range NOE connectivities involving NH, Hα, and Hβ protons indicated that the CsrA monomer is composed of five β-strands and a short α-helix. The unstructured C terminus is unfolded as shown by measurement of backbone $\{^1H\}$-^{15}N heteronuclear NOEs (Fig. 2E). Analysis of ^{13}C-edited NOESY experiments recorded in conjunction with and without carbon decoupling on a 1:1 mixture of $^{13}C/^{15}N$-labeled/nonlabeled CsrA allowed us to determine intermolecular NOEs and the hydrogen bond network defining the CsrA dimer (Fig. 1C).

Even though 95% of backbone and side chain resonances were unambiguously determined, assignment of NOE cross-peaks was challenging and ambiguous at several points. For instance, the core region of the protein is rich in valine residues (~20%), with proton and carbon nuclei resonating within a narrow chemical shift range. The dimeric nature of CsrA contributed further to this ambiguity. However, the high content of an antiparallel β-sheet within CsrA allowed the structure of CsrA to be defined using relatively sparse NMR-derived restraints (Fig. 2 and Table 1).

Each CsrA monomer is composed of five strands, β1 to β5, corresponding to residues 2 to 6, 10 to 15, 18 to 23, 30 to 35, and 41 to 43. Residues 46 to 50 fold into a short α-helix followed by an unstructured C terminus (residues 51 to 61). In the dimer, strands β1 and β5 of one monomer hydrogen bond to β4′ and β2′ of the other monomer, forming a mixed antiparallel β-sheet (Fig. 2B to D). Packing of these two mixed β-sheets forms the core of CsrA.

In spite of the low sequence similarity, it was proposed that CsrA was a member of the KH domain family, a group that comprises a diverse series of RNA-binding proteins (18). The characteristic signature of this protein family is the presence of a ~30-amino-acid segment that expands around a conserved GxxG core sequence (where x is any amino acid, with a preference for basic residues) (1). In CsrA, the GxxG motif has the sequence GVKG (residues 24 to 27) and is located in the loop connecting strands β3 and β4. Our structure proves that CsrA is not a member of the KH family of proteins, which have a characteristic βααββα topology (19, 20) that differs from that of CsrA. However, it is still likely that the GxxG sequence in CsrA is involved in the recognition of the GGA triplet present in all CsrA-binding sites (3).

RNA binding of CsrA. Charged residues in CsrA are grouped into well-defined clusters on the protein surface (Fig. 3A). The main basic patch comprises residues R6, R7, K26, R31, and the side chain amides of N28 and Q29, defining a putative RNA-binding site. Residues E10, E45, and E46 and D16, E17, and E39 give rise to well-defined acidic patches located on the side and bottom of the CsrA molecule. Electrostatic interactions between these basic and acidic patches may explain CsrA aggregation at high concentrations.

In order to map the RNA-binding surface of CsrA, we acquired HSQC spectra of the ^{15}N-enriched protein in the presence of different target RNAs. Based on the CAP leader mRNA sequence and the CsrB consensus, three different RNAs containing the GGA sequence were designed: glgC25 (ACCUGCACACGGAUUGUGUGGUUC), glgC15 (CACACGGAUUGUGUG), and a CsrB consensus heptamer (CAGGAUG) (GGA, the most conserved element of the consensus for CsrA binding, is underlined). As low pH could alter the protonation state of the nucleotide bases, therefore affecting

TABLE 1. Structural statistics for CsrA

Parameter[a]	Value
Constraints used for structure calculation	
Intraresidue NOEs ($n = 0$)	254
Sequential-range NOEs ($n = 1$)	74
Medium-range NOEs ($n = 2, 3, 4$)	22
Long-range NOEs ($n > 4$)	68
Intermolecular NOEs	78
Dihedral angle constraints	110
Hydrogen bonds	46
^{15}H-^1H residual dipolar couplings	104
Total no. of constraints	756
Final energies (kcal/mol)	
E_{total}	163.03 ± 4.52
E_{bond}	5.18 ± 0.51
E_{angle}	62.89 ± 1.99
$E_{improper}$	5.85 ± 0.93
E_{VdW}	2.10 ± 0.70
E_{noe}	13.70 ± 1.59
$E_{dihedral}$	2.10 ± 0.70
E_{sani}	34.82 ± 5.32
Deviations from idealized geometry	
Bonds (Å)	0.0016 ± 0.0001
Angles (°)	0.3401 ± 0.0054
Impropers (°)	0.1991 ± 0.0157
RMSD from experimental restraints	
Distance restraints (Å)	0.0183 ± 0.0011
Dihedral angle restraints (°)	0.4144 ± 0.0671
RMSD of the 20 structures from the mean coordinates (Å)	
Backbone atoms	0.5422 ± 0.1919
All heavy (nonhydrogen) atoms	1.1434 ± 0.2313
All atoms	1.4072 ± 0.1919
Average Ramachandran statistics for structured regions (%)	
Residues in most favored regions	82.57
Residues in additional allowed regions	16.36
Residues in generously allowed regions	1.07
Residues in disallowed regions	0.00
Analysis of residual dipolar couplings	
RMSD (Hz)	1.0280 ± 0.085
Q factor	0.1319 ± 0.011

[a] RMSD, root mean square deviation.

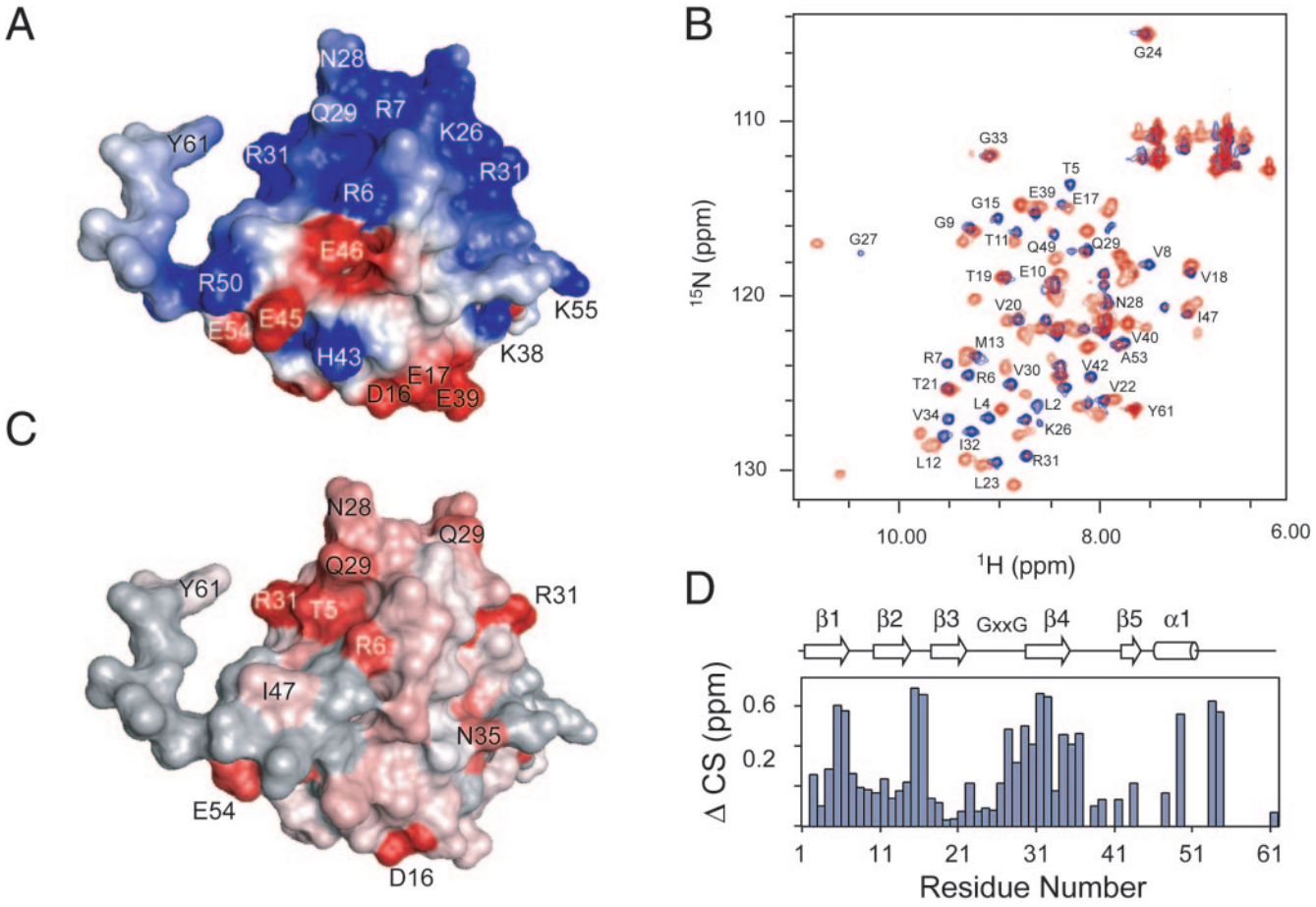

FIG. 3. Surface properties of CsrA. (A) Surface potential of the CsrA structure. Blue and red colors indicate positive and negative electrostatic potential, respectively. (B) Superposition of ^{15}N-HSQC spectra of CsrA in the absence (blue) and presence (red) of the glg15 RNA (5′-CACA CGGAUUGUGUG-3′). (C) Mapping of chemical shift changes (from panel D) onto the CsrA structure. Residues with large chemical shift changes are red or pink, residues with small changes are white, and residues that could not be quantified are gray. (D) Measured chemical shift changes versus residue number from the RNA titration, calculated using the equation $[(\Delta H)^2 + (0.2 \cdot \Delta N)^2]^{1/2}$. Secondary structural elements are shown on top. Blank spaces represent peaks that could not be traced with certainty.

RNA recognition, binding experiments were performed at pH 7.5. Titrations with both the glgC25 and glgC15 hairpin showed high-affinity binding as indicated by the slow exchange on the NMR time scale between bound and unbound forms. Binding of glgC25 and glgC15 affected almost all the CsrA amide signals, suggesting a large conformational change and/or major protein-RNA interactions upon RNA binding (Fig. 3B). Surprisingly, the CsrB consensus sequence caused no chemical shift perturbations. Unlike glgC25 and glgC15, which are predicted to form hairpin structures, the CsrB consensus is expected to be single stranded (3). It is possible that CsrA's affinity for RNA is greatly reduced when the RNA is not duplex. These results are consistent with previous reports showing that CsrA binds to the GGC sequence with higher affinity if it is part of a hairpin loop (3). Titration data mapped into the CsrA structure (Fig. 3C and D), suggesting that the loops connecting β1-β2, β3-β4 (GxxG motif), strand β4, and the C terminus are the regions responsible for RNA binding. In CsrA, the conserved and surface-exposed residues R6, R7, E10, N28, Q29, V30, and R31 are probably the ones most involved in recognizing the GGA RNA signature.

Toeprint analyses have identified the position of bound CsrA on target mRNAs (3, 11). In the case of the glgCAP transcript, RNA digestion and gel mobility assays were performed on a 134-nucleotide untranslated leader containing the CsrA-binding site. Binding of CsrA protected both the single-stranded glgC Shine-Dalgarno (SD) sequence and the glgCAP hairpin further upstream from cleavage by RNase T1 and Pb^{2+} (3). Structural changes seem to occur in the hairpin RNA, as CsrA binding enhanced the cleavage of the sequence in the stem-loop protected in the unbound form.

In light of our structural data, we postulate that the CsrA dimer presents its GxxG motif to simultaneously recognize both GGA sequences in the SD sequence and the upstream hairpin loop. Since SD sequences are present in most bacterial mRNAs, CsrA likely requires two signals to recognize the correct transcripts to be regulated. The upstream hairpin loop in glgCAP transcript may act as an allosteric activator for CsrA

binding to the downstream SD sequence. Further, CsrA seems to bind the GGA sequence with higher affinity when present as part of a hairpin loop than in single-stranded sequences. This is supported by experiments with reverse transcriptase where the SD-CsrA interaction was not sufficiently strong to disrupt the reverse transcriptase complex (3). Our titration experiments substantiate the finding that CsrA binds preferentially to hairpin loop structures. In addition, the GGA sequence in the hairpin loop affects the affinity of CsrA binding to the SD (3). Furthermore, conformational changes seem to occur upon binding to RNA as evidenced by our own data and footprinting studies and RNA structure mapping that demonstrated that the base of the glgCAP leader RNA hairpin is disrupted when CsrA is bound (3). Binding affinity is probably higher for the hairpin due to the reduced conformational entropy associated with this structure.

We propose that CsrA binds to its target mRNAs in two steps. First, the CsrA dimer recognizes the hairpin loop upstream of the SD and binds to the GGA sequence by using one of the GxxG loops. At this point, it is likely that both RNA and CsrA experience a conformational change that increases CsrA's affinity for the downstream single-stranded SD sequence. CsrA then binds to the SD sequence through the second GxxG motif, thereby preventing transcription and rendering the RNA more susceptible to degradation.

Note. While this paper was under review, the X-ray structure of the CsrA homolog from *P. aeruginosa* was released (RCSB PDB code 1VPZ). The structures are very similar (RMSD of 1.71 and a Dali *Z*-score of 10.0) and have identical strand topologies.

ACKNOWLEDGMENTS

This work was funded by Canadian Institutes of Health Research Genomics grant GSP-48370 (M. Cygler and K. Gehring) and by the Ontario Research and Development Challenge Fund and Genome Canada (C. H. Arrowsmith and A. M. Edwards). K.G. is a Chercheur National of the fonds de la recherché en santé Québec.

We thank M. Cygler, M. Bachetti, D. Elias, G. Kozlov, T. Moldovenau, and N. Siddiqui for assistance and helpful discussions.

REFERENCES

1. **Adinolfi, S., C. Bagni, M. A. Castiglione Morelli, F. Fraternali, G. Musco, and A. Pastore.** 1999. Novel RNA-binding motif: the KH module. Biopolymers **51:**153–164.
2. **Altier, C., M. Suyemoto, and S. D. Lawhon.** 2000. Regulation of *Salmonella enterica* serovar Typhimurium invasion genes by *csrA*. Infect. Immun. **68:** 6790–6797.
3. **Baker, C. S., I. Morozov, K. Suzuki, T. Romeo, and P. Babitzke.** 2002. CsrA regulates glycogen biosynthesis by preventing translation of glgC in Escherichia coli. Mol. Microbiol. **44:**1599–1610.
4. **Brunger, A. T., P. D. Adams, G. M. Clore, W. L. DeLano, P. Gros, R. W. Grosse-Kunstleve, J. S. Jiang, J. Kuszewski, M. Nilges, N. S. Pannu, R. J. Read, L. M. Rice, T. Simonson, and G. L. Warren.** 1998. Crystallography & NMR system: a new software suite for macromolecular structure determination. Acta Crystallogr. D **54:**905–921.
5. **Clore, G. M., A. M. Gronenborn, and A. Bax.** 1998. A robust method for determining the magnitude of the fully asymmetric alignment tensor of oriented macromolecules in the absence of structural information. J. Magn. Reson. **133:**216–221.
6. **Clore, G. M., A. M. Gronenborn, and N. Tjandra.** 1998. Direct structure refinement against residual dipolar couplings in the presence of rhombicity of unknown magnitude. J. Magn. Reson. **131:**159–162.
7. **Cornilescu, G., F. Delaglio, and A. Bax.** 1999. Protein backbone angle restraints from searching a database for chemical shift and sequence homology. J. Biomol. NMR **13:**289–302.
8. **Cui, Y., A. Chatterjee, Y. Liu, C. K. Dumenyo, and A. K. Chatterjee.** 1995. Identification of a global repressor gene, *rsmA*, of *Erwinia carotovora* subsp. *carotovora* that controls extracellular enzymes, *N*-(3-oxohexanoyl)-L-homoserine lactone, and pathogenicity in soft-rotting *Erwinia* spp. J. Bacteriol. **177:**5108–5115.
9. **Cui, Y., A. Mukherjee, C. K. Dumenyo, Y. Liu, and A. K. Chatterjee.** 1999. *rsmC* of the soft-rotting bacterium *Erwinia carotovora* subsp. *carotovora* negatively controls extracellular enzyme and $Harpin_{Ecc}$ production and virulence by modulating levels of regulatory RNA (*rsmB*) and RNA-binding protein (RsmA). J. Bacteriol. **181:**6042–6052.
10. **Delaglio, F., S. Grzesiek, G. W. Vuister, G. Zhu, J. Pfeifer, and A. Bax.** 1995. NMRPipe: a multidimensional spectral processing system based on UNIX pipes. J. Biomol. NMR **6:**277–293.
11. **Dubey, A. K., C. S. Baker, K. Suzuki, A. D. Jones, P. Pandit, T. Romeo, and P. Babitzke.** 2003. CsrA regulates translation of the *Escherichia coli* carbon starvation gene, *cstA*, by blocking ribosome access to the *cstA* transcript. J. Bacteriol. **185:**4450–4460.
12. **Ekiel, I., M. Abrahamson, D. B. Fulton, P. Lindahl, A. C. Storer, W. Levadoux, M. Lafrance, S. Labelle, Y. Pomerleau, D. Groleau, L. LeSauteur, and K. Gehring.** 1997. NMR structural studies of human cystatin C dimers and monomers. J. Mol. Biol. **271:**266–277.
13. **Gudapaty, S., K. Suzuki, X. Wang, P. Babitzke, and T. Romeo.** 2001. Regulatory interactions of Csr components: the RNA binding protein CsrA activates *csrB* transcription in *Escherichia coli*. J. Bacteriol. **183:**6017–6027.
14. **Jackson, D. W., K. Suzuki, L. Oakford, J. W. Simecka, M. E. Hart, and T. Romeo.** 2002. Biofilm formation and dispersal under the influence of the global regulator CsrA of *Escherichia coli*. J. Bacteriol. **184:**290–301.
15. **Johnson, B. A., and R. A. Blevins.** 1994. NMRView: a computer program for the visualization and analysis of NMR data. J. Biomol. NMR **4:**603–614.
16. **Laskowski, R. A., M. W. MacArthur, D. S. Moss, and J. M. Thornton.** 1993. PROCHECK: a program to check the stereochemical quality of protein structures. J. Appl. Crystallogr. **26:**283–291.
17. **Liu, M. Y., and T. Romeo.** 1997. The global regulator CsrA of *Escherichia coli* is a specific mRNA-binding protein. J. Bacteriol. **179:**4639–4642.
18. **Liu, M. Y., H. Yang, and T. Romeo.** 1995. The product of the pleiotropic *Escherichia coli* gene *csrA* modulates glycogen biosynthesis via effects on mRNA stability. J. Bacteriol. **177:**2663–2672.
19. **Musco, G., A. Kharrat, G. Stier, F. Fraternali, T. J. Gibson, M. Nilges, and A. Pastore.** 1997. The solution structure of the first KH domain of FMR1, the protein responsible for the fragile X syndrome. Nat. Struct. Biol. **4:**712–716.
20. **Musco, G., G. Stier, C. Joseph, M. A. Castiglione Morelli, M. Nilges, T. J. Gibson, and A. Pastore.** 1996. Three-dimensional structure and stability of the KH domain: molecular insights into the fragile X syndrome. Cell **85:** 237–245.
21. **Nilges, M., M. J. Macias, S. I. O'Donoghue, and H. Oschkinat.** 1997. Automated NOESY interpretation with ambiguous distance restraints: the refined NMR solution structure of the pleckstrin homology domain from beta-spectrin. J. Mol. Biol. **269:**408–422.
22. **Romeo, T.** 1998. Global regulation by the small RNA-binding protein CsrA and the non-coding RNA molecule CsrB. Mol. Microbiol. **29:**1321–1330.
23. **Romeo, T., M. Gong, M. Y. Liu, and A. M. Brun-Zinkernagel.** 1993. Identification and molecular characterization of *csrA*, a pleiotropic gene from *Escherichia coli* that affects glycogen biosynthesis, gluconeogenesis, cell size, and surface properties. J. Bacteriol. **175:**4744–4755.
24. **Rückert, M., and G. Otting.** 2000. Alignment of biological macromolecules in novel nonionic liquid crystalline media for NMR experiments. J. Am. Chem. Soc. **122:**7793–7797.
25. **Sabnis, N. A., H. Yang, and T. Romeo.** 1995. Pleiotropic regulation of central carbohydrate metabolism in Escherichia coli via the gene csrA. J. Biol. Chem. **270:**29096–29104.
26. **Wei, B., S. Shin, D. LaPorte, A. J. Wolfe, and T. Romeo.** 2000. Global regulatory mutations in *csrA* and *rpoS* cause severe central carbon stress in *Escherichia coli* in the presence of acetate. J. Bacteriol. **182:**1632–1640.
27. **Wei, B. L., A. M. Brun-Zinkernagel, J. W. Simecka, B. M. Pruss, P. Babitzke, and T. Romeo.** 2001. Positive regulation of motility and flhDC expression by the RNA-binding protein CsrA of Escherichia coli. Mol. Microbiol. **40:**245–256.
28. **Weilbacher, T., K. Suzuki, A. K. Dubey, X. Wang, S. Gudapaty, I. Morozov, C. S. Baker, D. Georgellis, P. Babitzke, and T. Romeo.** 2003. A novel sRNA component of the carbon storage regulatory system of Escherichia coli. Mol. Microbiol. **48:**657–670.
29. **Wishart, D. S., B. D. Sykes, and F. M. Richards.** 1991. Simple techniques for the quantification of protein secondary structure by ^{1}H NMR spectroscopy. FEBS Lett. **293:**72–80.